

INVESTIGATION INTO THE MECHANISMS OF HEAVY OIL RECOVERY BY WATERFLOODING AND ALKALI-SURFACTANT FLOODING

A. Mai., J. Bryan, A. Kantzas
University of Calgary, Canada

This paper was prepared for presentation at the International Symposium of the Society of Core Analysts held in Calgary, Canada, 10 – 12 September, 2007

ABSTRACT

The oil sands in northern Canada are characterized by unconsolidated high porosity, high permeability sands, containing highly viscous oil. Issues regarding how this viscous oil flows in porous media are paramount to its production. Heavy oil reservoirs are a subset of the oil sands, whereby the oil in place has some limited mobility at reservoir conditions. Limited studies have shown that waterflooding and alkali-surfactant flooding can lead to recovery of additional heavy oil, despite adverse injection mobility ratios. In this work, core flooding data are presented for a high viscosity heavy oil, in different permeability sands and under varying water injection rates. NMR spectra are interpreted to understand the effects of viscous and capillary forces in heavy oil systems, and to investigate the location of the injected water as a function of time. Alkali-surfactant (AS) flooding is also investigated as a follow-up to waterflooding, and the effect of emulsification is observed. This work presents both an investigation into heavy oil non-thermal recovery and also NMR interpretation of heavy oil floods.

INTRODUCTION

The Canadian deposits of heavy oil and bitumen are some of the largest in the world. These oil sands will play an important role in helping Canada to remain an important energy source for the world in future generations. Heavy oil is a special class of this unconventional oil that has viscosity ranging from 50 – 50,000 mPa·s. Heavy oil reservoirs are often found in high porosity, high permeability, unconsolidated sand deposits. At reservoir conditions, the oil may contain dissolved solution gas, thus some oil can be initially recovered using the energy from heavy oil solution gas drive. At the end of primary production, however, a significant fraction of oil still exists for potential secondary recovery. Many of these reservoirs are small and thin or segmented, making them poor candidates for expensive thermal or hydrocarbon solvent enhanced oil recovery strategies. In this work, laboratory investigations are carried out to investigate the potential for waterflooding and alkali-surfactant (AS) flooding of heavy oil.

Waterflooding of oil reservoirs is a well-recognized technique for oil recovery, and waterflooding theory for conventional oils has been well documented. The inherent assumption in conventional oil waterflooding theory is a similarity in viscosity between

oil and water [Dong and Dullien, 1999]. In heavy oil applications this is not the case, however practitioners often still attempt to apply the same theoretical understanding to their fields. There has been some limited experience documented for waterfloods in heavy oil reservoirs [Jennings, 1996; Kumar et al., 2005; Miller, 2006], but in general the mechanism of viscous oil recovery by waterflooding has not been explored. Waterflood recoveries are known to be low for high viscosity heavy oil, due to the adverse mobility ratio between oil and injected water. Despite the presumed inefficiency of this process, waterflooding is still commonly applied in many heavy oil fields since it is relatively inexpensive and field operators are experienced in designing and controlling waterfloods.

At the end of a conventional oil waterflood, residual oil is left in place due to reservoir heterogeneities or capillary trapping. In laboratory core flood experiments, capillary bypassing and snap-off are the main mechanisms responsible for trapping of oil [Chatzis et al., 1982]. In these reservoirs, however, the high oil viscosity (poor mobility ratio between displacing and displaced fluids) is the main cause for oil bypassing and residual oil at the end of the waterflood. Previous investigations have therefore focused on the mobility ratio and how it relates to viscous fingering or instability of the displacing water front. After water breakthrough, however, it is unclear how oil is still produced. Eventually, the majority of injected water will simply flow along the water pathways, and at low system pressures there is very little driving force for viscous oil to flow as well. This work utilizes the results from core floods and low field NMR to investigate water imbibition as the mechanism responsible for oil recovery after water breakthrough.

Even if waterfloods are controlled such that capillary forces can be utilized, some oil will still not be recovered due to the adverse oil-water mobility ratio. At the end of waterflooding, therefore, there still exists potential for additional oil recovery by alkali-surfactant (AS) flooding. AS flooding is the process of injecting alkali and pre-formed surfactant into a reservoir. Alkali solutions react with acids in the oil to form *in-situ* surfactants, and the process is made more stable by the co-injection of additional preformed surfactant. Surfactants are a special class of molecules that tend to align themselves at the oil-water interface, which can lead to dramatic reductions in interfacial tension [Garrett, 1972]. In conventional oil, this leads to reduced capillary trapping of oil. For AS floods to be successful in heavy oil, the injected chemical must somehow be improving the mobility ratio.

It has been shown in previous work [Johnson, 1976; Farouq Ali et al., 1979; Liu et al., 2006; Bryan and Kantzas, 2007] that when caustic or preformed surfactants are injected into oil reservoirs, this can also lead to the generation of emulsions. Oil-in-water emulsions, specifically, have potential for recovery of heavy oil. When water is the continuous phase, the resulting emulsion viscosity is considerably lower than that of the oil [McAuliffe, 1973], thus if oil can be emulsified into water, the oil can possibly be recovered at least partially by being entrained in the water phase, and flowing as a low viscosity oil-in-water emulsion. This is the mechanism of emulsification and entrainment summarized by Johnson (1976). In this work, alkali and preformed surfactant are

injected into sand packs containing dead (gas-free) heavy oil. The pressures and the produced fluids are monitored for evidence of emulsion formation, and the *in-situ* oil and water saturation are measured as a function of length using low field NMR.

WATER IMBIBITION EXPERIMENTS

In previous work [Mai and Kantzas, 2007] it was observed that over the entire course of a waterflood, oil recovery was affected by oil viscosity, water injection rate and sand permeability. Experiments were performed at varying rates, and the rates and pressures were normalized in order to remove the effect of the viscous forces from the oil rates. It was observed that even after normalization, the oil flow rates were higher at lower injection rates, and this effect was more pronounced in lower permeability cores. Therefore, it was postulated that this was evidence for oil recovery by water imbibition. In this work, low field NMR was utilized to obtain further evidence of this mechanism in static and flowing systems.

Water Imbibition in Static Vials

The purpose of this experiment was to establish whether imbibition could be monitored using NMR. NMR is capable of detecting the presence and position of fluids in a porous medium, thus it was used to monitor the distribution of oil and water. The distribution of fluids is controlled by wettability of the sand. If the sand is water wet, water will move into the small pores with oil existing in the large pores. Thus, if water spectra shift to faster relaxation times, this is evidence of a water wet rock and water imbibition.

The sand used in this experiment was Lane Mountain 70, which has a fairly narrow range of pore sizes and only a small fraction of very fine grains (resulting in small pores). Approximately 80% of the sand is in the range of 150 – 250 μm . The spectrum of the sand saturated with brine is shown in Figure 1. This figure shows that surface bound water exists in a broad peak between 100 – 1000 ms, and another small peak under 10 ms. The bulk brine is a low viscosity fluid, having a narrow peak at around 2000 ms, while bulk oil has a fast-relaxing broad peak under 10 ms. When the oil is in sand, the relaxation times are essentially unchanged due to the high oil viscosity.

From prior knowledge of the porosity and initial water saturation, an appropriate amount of oil was homogeneously mixed with sand. The mixture was then divided into equal portions and packed into four glass vials, labeled as A – D. The oil and sand was compacted manually, but no overburden was applied. Small amounts of brine were then added to each vial and periodically NMR measurements were obtained. The brine initially existed as a bulk phase on top of the oil and sand mixture, and manifested itself as a peak at high T_2 values (~ 1000 ms). If the sand is water wet, water should imbibe into the small pores first, but this is not readily apparent upon examination of the spectra due to the presence of the oil signal at early relaxation times. Fortunately, the NMR spectra of two different vials had been obtained prior to brine addition. The spectra of these two vials before and immediately after brine addition are shown in Figure 2. Brine addition led to increases in the amplitude of the first peak, indicating that brine did in fact

occupy the small pores, and that the sand is water wet. Brine imbibition into small pores occurred despite the fact that the sand was originally coated with oil.

Further evidence of imbibition could also be seen from the NMR spectra measured with time. Figure 3 shows the shift in the NMR spectra of vial C over 1702 hrs. Throughout the experiment, the weights of the vials were obtained to monitor evaporation. The change in weights was insignificant, thus evaporation is not responsible for changes in the spectra. In Figure 3 the signal of the bulk brine shifts to smaller T_2 , under 1000 ms, indicating that the original bulk brine is gradually invading the porous medium and surface relaxation is causing enhanced relaxation rates. This shift in the spectra could be described by plotting the geometric mean of the water signal at $T_2 > 10$ ms, as shown in Figure 4. Water T_{2gm} values decreased with time for all four vials. In a closed system, if water moves into the pores, then oil must be transferred either into larger pores or be expelled out of the sand. This redistribution of fluids is a direct indication that imbibition occurs in this water wet sand.

At the end of the experiment, in the vials where there was excess water (i.e. the amount of brine originally added is greater than the pore space) a layer of oil was observed above the oil, sand and water. Despite the lower oil density (0.9815 g/cm^3), gravitational forces were not responsible for the fluid redistribution in the porous medium. This was concluded through the calculation of the Bond number, which is a ratio of gravitational to capillary forces. In this experiment, the Bond number is approximately 4.7×10^{-6} , indicating that the gravitational forces are negligible in the porous medium, and capillary forces alone are responsible for fluid re-distribution in the sand.

NMR Spectra of Heavy Oil Waterfloods

The experiments in a closed system (static vials) provided evidence that the sand used in this study is water wet and imbibition can lead to fluid redistribution, which can in turn cause oil production from the porous medium. The important question that had to be answered, however, is whether imbibition is still significant during flow of heavy oil, and whether this can aid in the recovery of heavy oil in waterflooding. Several waterfloods were therefore carried out using the same sand and fluids as in the static vials.

In the waterfloods, the sand was wet-packed into a PEEK core-holder. PEEK is a high performance non-magnetic plastic that can withstand high injection pressures. The core was first packed with sand, and then was dried and its porosity was determined. The core was then saturated with brine and the permeability to brine was measured. Next, oil was injected until the irreducible water saturation was reached. Water was then injected at fixed injection rates, and NMR spectra were obtained over time to monitor the location of the water at different times in the waterflood. NMR measurements were performed using an Ecotek FTB relaxometer, which operates at a frequency of around 1.8 MHz, using an echo spacing of 0.16 ms. The core used has a length of around 9.3 cm and a diameter of 2.54 cm. The rock porosity and permeability are approximately 0.46 and 14 D, respectively. The viscosity of the heavy oil used in these waterfloods is 11 500 mPa.s.

Floods were performed at two fixed flow rates (8.89 and 0.45 cm³/hr), however due to space limitations in this paper only the spectra of the injection rate of 0.45 cm³/hr (0.021 m/day) are presented.

The spectra obtained prior to the start of the oil production in the closed system and in waterflooding case are compared in Figure 5 (a). The condition at the beginning of these experiments was very different. In the closed system, oil originally coated the sand grains and brine was introduced as a bulk phase on top of the sand and oil mixture. In the core, the sand grains were coated with water so the irreducible water exists at faster relaxation times than in the static vials. The spectra of the core fully saturated with water and at S_{wi} are compared in Figure 5 (b). During oil saturation, water was displaced out of the large pores, shown by the disappearance of the water peak at 500 ms. NMR spectra were obtained as the waterflood progressed, and some are shown in Figure 6. It can be seen that the water peak grew first at high T_2 , meaning that water is displacing the oil in the large pores. This indicates the dominance of viscous forces at early time [Mai and Kantzas, 2007]. The NMR spectra also show evidence of imbibition as time progresses, in which the second peak slowly shifted to lower values with time.

Figure 7 shows the production profile for both constant rate waterfloods. As expected for adverse mobility ratio floods, the recovery at the lower injection rate is significantly better than at high injection rates. The water amplitude fractions (amplitude after the first peak divided by total amplitude) for both injection rates are shown in Figure 8. The assumption made in this figure is that water amplitude is the signal after the first peak, thus the first peak is assumed to be the oil amplitude. In this manner, the water amplitude fraction is analogous to the water saturation at any given time. Surprisingly, the water amplitude fraction is actually much higher for the fast injection rate, which would mean a higher oil recovery at this rate. This is counter-intuitive, and is not supported by the measured production data in Figure 7. Additionally, at the low injection rate the water amplitude fraction appears to level off at around 0.15, while the measured oil recovery in Figure 7 continuously increases.

The data from Figures 7 and 8 can only be reconciled if some of the assumed oil amplitude in the first peak of the NMR spectra is actually the contribution of fast-relaxing water. Water relaxing this quickly must be in more constricted spaces than in the original core, as shown by the lack of significant water signal at such early times when the core was fully saturated with water (Figure 5). This indicates the presence of a significant portion of water relaxing in water films, which have larger surface-to-volume ratios than pores fully saturated with water. At the lower injection rate, therefore, some of the water present in the porous medium exists as thickening films, which is evidence of imbibition occurring. Imbibition is a slow process, especially in high viscosity heavy oils, which is why its effect is more significant at lower injection rates, where the time for several pore volumes to be injected is much longer than at fast injection rates. The effect of the water in small pores is important, however, as evidenced by the much higher oil recovery at this

injection rate. This data demonstrates at low waterflood rates, imbibition can be significant, even under flowing conditions for heavy oil.

ALKALI-SURFACTANT FLOODING OF HEAVY OIL

The surfactant used in this study is a commercial anionic surfactant supplied by Stepan Oil Company. This surfactant (Bio-Terge PAS-8S) is a sodium alkane sulfonate. The alkali used in this study is sodium carbonate (Na_2CO_3). All surfactants are anionic, which indicates that electrostatic repulsion between negatively charged surfactant heads will lead to barriers to oil droplets coalescing. In this manner, O/W emulsions are theoretically possible even with high viscosity heavy oil [Acevedo et al., 2001]. The injected chemical solution consisted of 0.1 wt% surfactant and 0.5 wt% alkali. Therefore, the total injected fluid is still 99.4% water.

Studies from other researchers [Nelson et al., 1984] have shown a strong influence of salinity on emulsion type. In systems where the oil is much more viscous than the water, the salinity effect is much more pronounced. Bulk liquid studies performed previously [Bryan and Kantzas, 2007] indicated that if AS solutions were made in de-ionized (DI) water, oil-in-water (O/W) emulsions would form. In the presence of NaCl, water-in-oil (W/O) emulsions form preferentially. In this work, therefore, after waterflooding a DI AS flood was carried out in order to investigate if O/W emulsions could actually form and flow in porous media. The reason for these experiments is that other researchers [Liu et al., 2006] had previously observed O/W emulsification only in micromodel studies, but never in the effluent from laboratory core floods. At the end of the DI AS flood, an additional AS flood was performed in 2 wt% NaCl brine (Brn AS flood). In a brine flood, the W/O emulsions observed in the bulk liquid studies [Bryan and Kantzas, 2007] are more viscous than the constituent oil, thus these emulsions may lead to improved sweep efficiency and some further oil may be recovered.

The core holder used in this study was also made of PEEK, and has a diameter of 2.6 cm, with a length of 53 cm. The core was placed inside an Ecotek FT relaxometer, which operates at a frequency of around 1.9 MHz and the same echo spacing of 0.16 ms. The sand used in this core was a sieved fraction of the sand in the previous experiments, and thus the core permeability is lower – 0.79 D. The same oil was used in these floods, and the sand pack was prepared in the same manner as in the small NMR core floods. This paper outlines the waterflood and AS flood response when floods were carried out at a constant velocity of 0.51 m/day.

Figure 9 shows the saturation as a function of length, determined from NMR, for the core at different states. During DI AS injection, the water saturation increases above the waterflood saturation along the entire length of the core. At the end of the flood the water saturation is relatively constant all along the core. After waterflooding for five pore volumes, the average water saturation was 0.291. DI AS was injected for just over one pore volume and the average water saturation increased to 0.345. Thus an additional 5.5% of oil was recovered by the injection of AS solution. After DI AS flooding, a brine

salinity buffer was injected, followed by another pore volume of Brn AS. After the Brn AS flood, the average water saturation was 0.403, so in total the addition of two pore volumes of AS solution led to the production of 11% additional oil. At the end of DI AS or Brn AS flooding the water saturation is relatively constant across the core. This is an important finding, as it means that oil is produced along the entire length of the system, and the improved response from AS flooding is not just a near-wellbore effect.

Figure 10 shows the measured pressure and production response obtained for the AS floods. Region A in Figure 10 is the DI AS flood and Region C is the Brn AS flood. In between floods the injection of the brine salinity buffer required only low pressures, and is denoted as Region B. At the start of the DI AS injection, pressure in the system had been declining during the waterflood. Upon injection of AS fluid, the pressure increased once again. While pressure increased, the produced fluid appeared to be water with only a small fraction of oil. After pressure peaked and began to decline, the produced fluid turned black and for the remainder of the flood the produced fluid appeared to be a low viscosity, black fluid. This is direct evidence of the production of an O/W emulsion, which proves that these emulsions can form *in-situ* and flow at normal flow rates. This result is important, as O/W emulsion formation and flow had only previously been inferred [Liu et al., 2006]. During Brn AS injection (Region C) the produced fluid consisted of clear water and a viscous oil phase. Pressure in the system increased again and stayed high throughout the duration of the Brn AS flood. These fluids were also more difficult to separate than the waterflood samples, which is an indication that high viscosity W/O emulsions had been produced.

Aside from providing information on fluid saturation as a function of length, the properties of the NMR spectra can also be used to identify the physical location of the oil and water in the pore space. Figure 11 (a) shows the oil and water spectra at the end of the DI AS flood, and water T_{2gm} values at different states are shown in Figure 11 (b). What is remarkable is that upon addition of AS to the system, a third water peak develops, close to the bulk value of water. In waterflooding or brine flooding, the water T_{2gm} values are all similar to that of the core fully saturated with water. In the presence of DI AS or Brn AS, however, the generation of this slow relaxing water peak leads to water T_{2gm} values that are slower than even the system containing no oil.

In order to properly interpret the response during AS flooding, the water spectra were split into surface components and bulk components. The bulk amplitude is the amplitude in the last peak, around 1000 ms. After waterflooding there is only a bulk peak present near to the inlet of the model, but at later sections of the core less than 10% of the water amplitude is bulk. After DI AS flooding, in the first half of the core the bulk amplitude fraction is very high (around 35% of the total water amplitude) and in the outlet section of the core the bulk amplitude is small again. After Brn AS flooding, the bulk amplitude peak is consistently high (30% of the total water amplitude) all along the length of the core.

After waterflooding and AS flooding, there was always still a significant portion of the water that was relaxing by surface relaxation (under 200 ms). However, it seems that the addition of chemical somehow leads to additional slower relaxation of water, as seen by the generation of the bulk water peak. Several factors can possibly be responsible for this slower relaxing water signal. One possibility is that the addition of alkali and surfactant somehow altered the rock surface relaxivity, reducing the effect of the surface relaxation. However, this cannot have happened, as there is still a significant surface relaxation peak even after AS addition (Figure 11). Additionally, during the brine flood before Brn AS injection, the water relaxation times become once again very similar to the waterflood and fully saturated spectra. Therefore, the presence of the bulk water signal indicates a physical difference in the water location in the rock pores.

During AS flooding, low interfacial tension can lead to the generation of O/W emulsions or W/O emulsions. If the emulsion is water-continuous, protons in the water can still relax against the pore walls, so this should not lead to slower water relaxation. The only thing that can cause slower water relaxation is if the water exists as a W/O emulsion. In this state, the water can no longer access the pore walls. This slow emulsion relaxation was also observed previously in the study of emulsion viscosity [Bryan et al., 2002]. Near to the entrance, therefore, the NMR spectra indicate that some W/O emulsions have formed even in DI AS floods, where O/W emulsions were produced. These emulsions block off the water channels, leading to increased pressure in the system. During this time, new pores are being accessed by the AS solution, thus mainly only the aqueous phase is produced. Eventually, water breaks through and pressure in the system declines again. The oil is displaced into the previously flooded channels and mixes with the DI AS solution, generating an O/W emulsion that is produced.

After Brn AS injection, there is a bulk water peak in the spectra of all lengths, indicating that W/O emulsions formed all along the core in the presence of NaCl. The pressure consistently stays high in this flood, indicating that as Brn AS solution moves into the core, it continuously generates new W/O emulsions. The mechanism of recovery by Brn AS injection is therefore different than that of O/W emulsion flow. In this flooding configuration, W/O emulsions constantly are plugging off water channels, leading to improved sweep in the core. The high pressures also indicate a reduced mobility to water, which again shows that Brn AS injection recovers oil through improved sweep.

CONCLUSIONS

NMR spectra of oil, water and sand mixtures indicate that water imbibition occurs during both static and flowing conditions, thus imbibition is at least partially responsible for oil production after water breakthrough. At low injection rates, a significant fraction of the water amplitude is found at fast relaxation times, which is evidence that capillary forces are significant even in viscous heavy oil systems, and can be used to improve oil recovery in adverse mobility conditions. In AS flooding experiments, it was observed that the addition of chemical leads to the generation of W/O emulsions, even if the observed

production mechanism is that of O/W emulsions being entrained in the water. In the presence of salt, only W/O emulsions form and can lead to improved sweep efficiency.

ACKNOWLEDGEMENTS

The authors wish to acknowledge the contributions of Xiao Dong Ji, Jun Gao and Michael Erath of TIPM Laboratory in helping with this project. The oil used in this study was generously provided by Nexen Inc., and the surfactant was provided by Stepan Oil Company. Financial support was received from NSERC, COURSE, ISEEE and the Canada Research Chair in Energy and Imaging and its Industrial Affiliates (Shell, Nexen, Devon, PetroCanada, Canadian Natural, ET Energy, Suncor, Schlumberger, Laricina, Paramount).

REFERENCES

- Acevedo, S., Gutierrez, X. and Rivas, H., "Bitumen-in-Water Emulsions Stabilized with Natural Surfactants", *J. Colloid and Interface Science*, **242**, 230 – 238, 2001.
- Bryan, J. and Kantzas, A., "Potential for Alkali-Surfactant Flooding in Heavy Oil Reservoirs Through Oil-in-Water Emulsification", CIM 2007-134, 58th Annual Technical Meeting of the Petroleum Society of CIM, Calgary, AB CANADA, June 12 – 14, 2007.
- Bryan, J., Kantzas, A. and Bellehumeur, C., "Using Low Field NMR to Predict Viscosities of Crude Oils and Crude Oil Emulsions", SCA Paper 2002-039, 2002 International Symposium of the Society of Core Analysts, Monterey, California USA, September 22 – 25, 2002.
- Chatzis, I., Morrow, N.R. and Lim, H.T., "Magnitude and Detailed Structure of Residual Oil Saturation", SPE/DOE 3rd Joint Symposium on Enhanced Oil Recovery, Tulsa, Oklahoma USA, April 4 – 7, 1982.
- Dong, M. and Dullien, F.A.L., "Effect of Capillary Forces on Immiscible Displacement in Porous Media", SPE 56676, SPE Annual Technical Conference and Exhibition, Houston, Texas USA, October 3 – 6, 1999.
- Farouq Ali, S.M., Figueroa, J.M., Azuaje, E.A., and Farquharson, R.G., "Recovery of Lloydminster and Morichal crudes by caustic, acid and emulsion floods", *J. Can. Pet. Tech.*, 53 – 59, January – March, 1979.
- Garrett, H.E., *Surface Active Chemicals*, Pergamon Press, 1972.
- Kumar, M., Hoang, V. and Satik, C., "High Mobility Ratio Waterflood Performance Prediction: Challenges and New Insights", SPE 97671, SPE International Improved Oil Recovery Conference, Kuala Lumpur, Malaysia, December 5 – 6, 2005.
- Jennings, H.Y., "Waterflood Behaviour of High Viscosity Crudes in Preserved Soft and Unconsolidated Cores", SPE 1202, *J. Pet. Tech.*, 116 – 120, January 1996.
- Johnson, C.E. Jr., "Status of Caustic and Emulsion Methods", SPE Paper 5561, *J. Pet. Tech.*, pg. 85 – 92, January 1976.
- Mai, A., Bryan, J. and Kantzas, A., "New Insights Into In-situ Measurements of Oil Sand Samples", SCA 2006-A68 (poster/extended abstract), International Symposium of the Society of Core Analysts, Trondheim, Norway, September 13 – 15, 2006.

Mai, A. and Kantzas, A., “Heavy Oil Waterflooding: Effects of Flow Rate and Oil Viscosity”, CIM 2007-144, 58th Annual Technical Meeting of the Petroleum Society of CIM, Calgary, AB CANADA, June 12 – 14, 2007.

McAuliffe, C.D., “Oil-in-Water Emulsions and Their Flow Properties in Porous Media”, *J. Pet. Tech.*, 727-733, 1973.

Miller, K.A., “Improving the State of the Art of Western Canadian Heavy Oil Waterflood Technology”, *J. Can. Pet. Tech.*, **45** (4), 7 – 11, 2006.

Liu, Q., Dong, M. and Ma, S., “Alkaline/Surfactant Flood Potential in Western Canadian Heavy Oil Reservoirs”, SPE 99791, 2006 SPE/DOE Symposium on Improved Oil Recovery, Tulsa, Oklahoma USA, April 22 – 26, 2006.

Nelson, R.C., Lawson, J.B., Thigpen, D.R. and Stegemeir, G.L., “Cosurfactant-Enhanced Alkaline Flooding”, SPE/DOE 12672, SPE/DOE 4th Symposium on Enhanced Oil Recovery, Tulsa, OK USA, April 15 – 18, 1984.

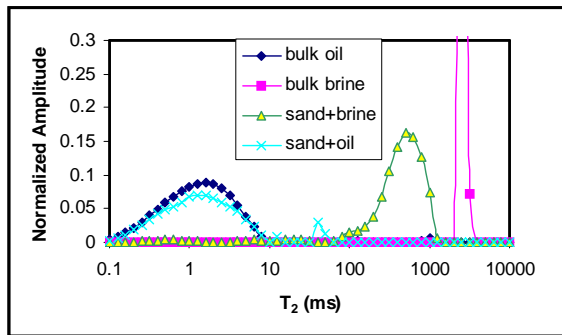


Figure 1. NMR spectra of various systems

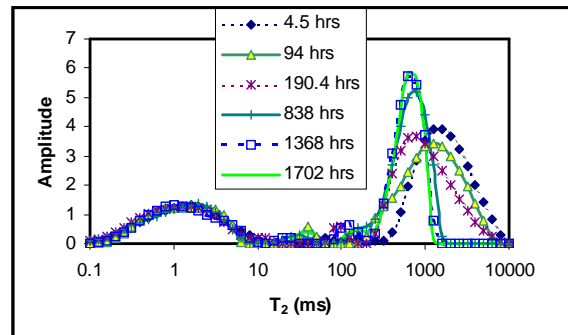


Figure 3. NMR spectra in static vials as a function of time

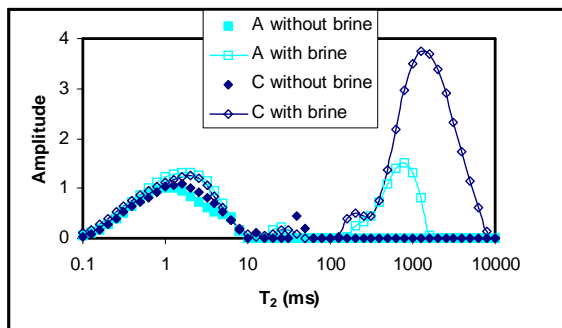


Figure 2. Spectra showing water imbibition in small pores

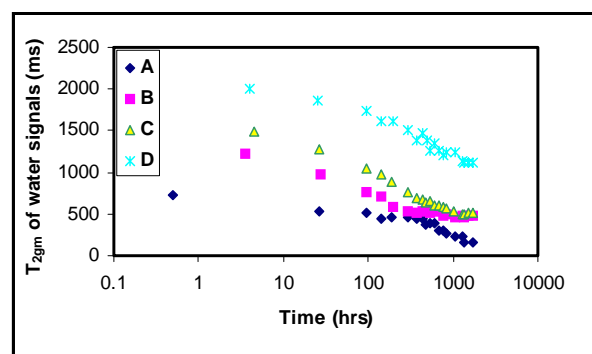


Figure 4. T_{2gm} of water signal after 10 ms as a function of time

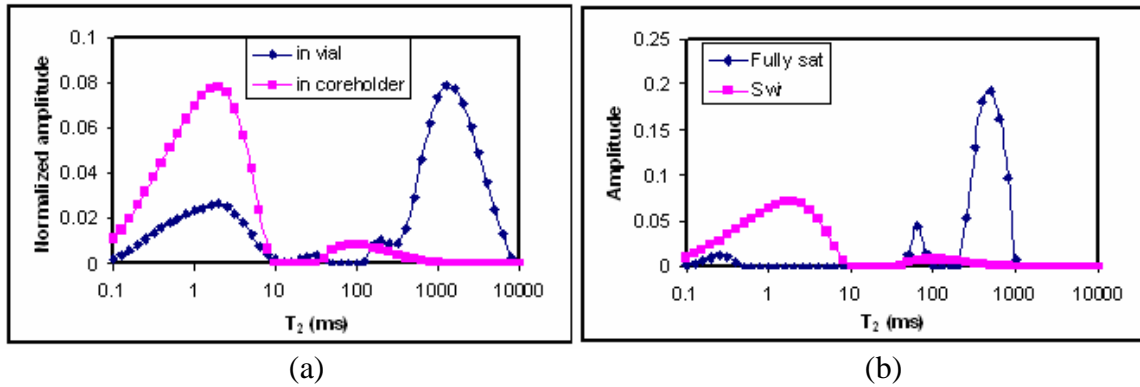


Figure 5. Spectra in static vial vs. core (a), and core spectra at different states (b)

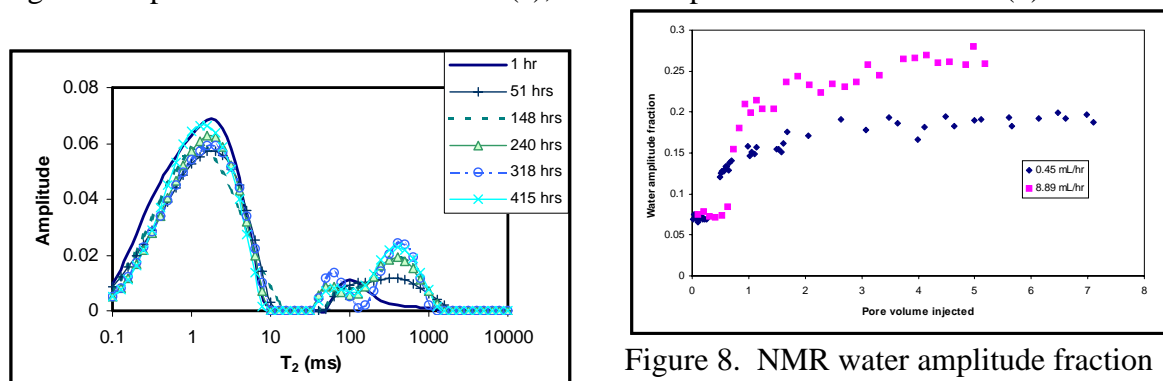


Figure 6. Changes in oil sand spectra with time

Figure 8. NMR water amplitude fraction for two water injection rates

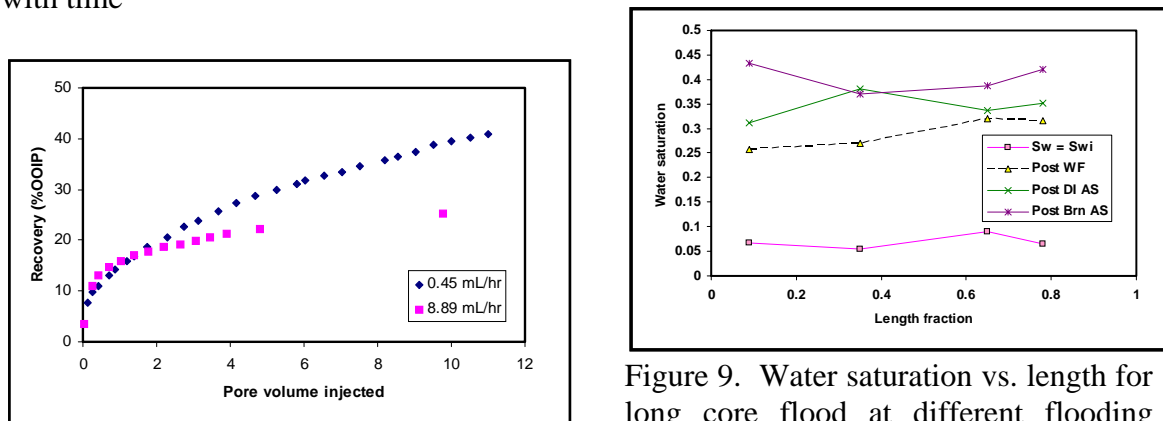


Figure 7. Measured oil recovery profile for two water injection rates

Figure 9. Water saturation vs. length for long core flood at different flooding stages

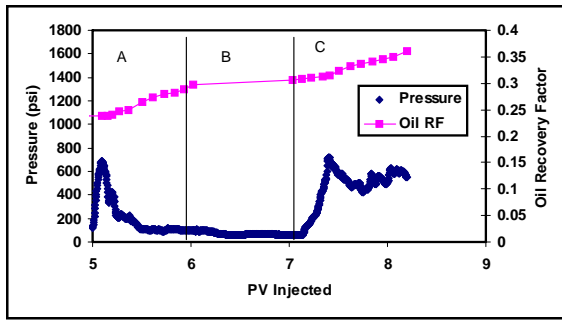
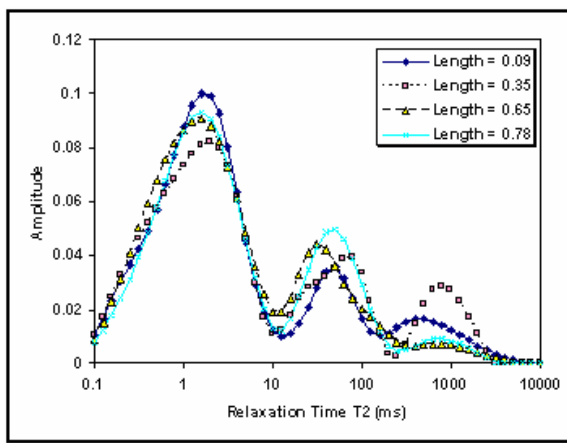
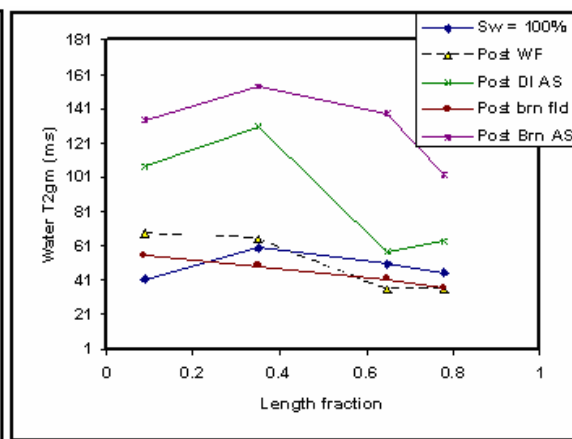


Figure 10. Pressure profile for DI AS flooding and Brn AS flooding



(a)



(b)

Figure 11. Spectra after AS Flooding (a) and Water T_{2gm} values at different states (b)